KIX8 and KIX9 are conserved repressors of organ size in the asterid species tomato

Gwen Swinnen[1,2], Alexandra Baekelandt[1,2], Rebecca De Clercq[1,2], Jan Van Doorsselaere[3], Nathalie Gonzalez[4], Dirk Inzé[1,2], Alain Goossens[1,2,*] and Laurens Pauwels[1,2,*]

[1]Ghent University, Department of Plant Biotechnology and Bioinformatics, 9052 Ghent, Belgium

[2]VIB Center for Plant Systems Biology, 9052 Ghent, Belgium

[3]VIVES, 8800 Roeselare, Belgium

[4]INRAE, Université de Bordeaux, BFP, 33882 Villenave d'Ornon Cedex, France

ORCID IDs: 0000-0002-4438-0098 (G.S.); 0000-0003-0816-7115 (A.B.); 0000-0002-4068-1811 (R.D.C.); 0000-0002-3768-2434 (J.V.D.); 0000-0002-3946-1758 (N.G.), 0000-0002-3217-8407 (D.I.); 0000-0002-1599-551X (A.G.); 0000-0002-0221-9052 (L.P.)

Corresponding authors:

Laurens Pauwels

VIB-UGent Center for Plant Systems Biology

Technologiepark 71, B-9052 Gent (Belgium)

Tel.: +32 9 331 39 71; Fax: +32 9 331 38 09

E-mail: laurens.pauwels@psb.vib-ugent.be

Alain Goossens

VIB-UGent Center for Plant Systems Biology

Technologiepark 71, B-9052 Gent (Belgium)

Tel.: +32 9 331 38 51; Fax: +32 9 331 38 09

E-mail: alain.goossens@psb.vib-ugent.be

Short title: KIX8 and KIX9 control tomato organ size

Keywords: Tomato, organ development, fruit size, *KIX*, *PPD*, CRISPR-Cas9, genome editing, crop improvement.

Summary

Plant organ size and shape are major agronomic traits that depend on cell division and expansion, which are tightly regulated by complex gene networks. In several eudicot species belonging to the rosid clade, organ growth is controlled by a repressor complex consisting of PEAPOD (PPD) and KINASE-INDUCIBLE DOMAIN INTERACTING (KIX) proteins. Whether the function of these proteins as regulators of organ size is conserved in asterids as well, which together with the rosids constitute most of the core eudicot species, is still unknown. Here, we demonstrate that KIX8 and KIX9 redundantly regulate organ growth in the asterid model species tomato (*Solanum lycopersicum*). Protein interaction assays in yeast revealed that KIX8 and KIX9 act as molecular bridges between the PPD repressor and TOPLESS co-repressor proteins. We found that CRISPR-Cas9 genome editing of *KIX8* and *KIX9* led to the production of enlarged, dome-shaped leaves and that these leaves exhibited increased expression of putative PPD target genes. Moreover, the *kix8 kix9* mutants carried bigger fruits with increased pericarp thickness. Our results show that KIX8 and KIX9 are conserved regulators of organ size in distinct eudicot species and can thus provide strategies to improve yield in fruit crops.

Introduction

Plants come in all shapes and sizes, yet these agronomically important traits are remarkably uniform within a given species or variety. Not surprisingly, cell division and cell expansion, the underlying processes of organ development, are under tight genetic control (Gonzalez *et al.*, 2012; Hepworth and Lenhard, 2014; Kalve *et al.*, 2014; Vercruysse *et al.*, 2020). The different phases of leaf development, for instance, are regulated by complex gene networks (Gonzalez *et al.*, 2012; Hepworth and Lenhard, 2014). Leaf development consists of the emergence of a leaf primordium from the shoot apical meristem, followed by a period of primary cell division that transitions into a cell expansion stage, and a simultaneous phase of meristemoid division. In Arabidopsis (*Arabidopsis thaliana*), the number of self-renewing asymmetric divisions that stem-cell like meristemoids can undergo before differentiating into stomatal guard cells is limited by a transcriptional repressor complex (Gonzalez *et al.*, 2015; White, 2006). This protein complex, which comprises PEAPOD 2 (PPD2) and KINASE-INDUCIBLE DOMAIN INTERACTING 8 (KIX8)/KIX9 (Figure S1a), thereby restricts leaf growth (Gonzalez *et al.*, 2015; White, 2006). KIX8 and KIX9 functionalities are required for the repressive activity of PPD2 (Gonzalez *et al.*, 2015). Consequently, double *kix8 kix9* knockout plants display

increased transcript levels of PPD2 target genes and enlarged, dome-shaped leaves because of a prolonged period of meristemoid division, similar as *ami-ppd* plants do (Gonzalez *et al.*, 2015).

In Arabidopsis, KIX8 and KIX9 can interact with both PPD1 and PPD2 (Gonzalez *et al.*, 2015). The PPD proteins, together with TIFY8 and the JASMONATE ZIM DOMAIN (JAZ) proteins, belong to class II of the TIFY protein family (Bai *et al.*, 2011; Vanholme *et al.*, 2007) and are characterized by the presence of a conserved TIF[F/Y]XG motif. This motif resides within the ZINC-FINGER PROTEIN EXPRESSED IN INFLORESCENCE MERISTEM (ZIM) domain that mediates the interaction of class II TIFY proteins with the transcriptional co-repressor NOVEL INTERACTOR OF JAZ (NINJA) (Figure S1a) (Baekelandt *et al.*, 2018; Chini *et al.*, 2009; Chung and Howe, 2009; Pauwels *et al.*, 2010). In contrast to class I members, class II proteins do not harbor a C2C2-GATA protein domain, but all of them, except TIFY8, do contain a C-terminal Jas domain (Bai *et al.*, 2011; Vanholme *et al.*, 2007). The Jas domain found in PPD proteins, however, is divergent from the Jas consensus motif in JAZ proteins (Bai *et al.*, 2011) that mediates the interaction of JAZ proteins with transcription factors such as MYC2 and the F-box protein CORONATINE INSENSITIVE 1 (COI1) (Chini *et al.*, 2007; Thines *et al.*, 2007). In addition, the PPD proteins contain a specific N-terminal PPD domain (Bai *et al.*, 2011) that facilitates their interaction with KIX8 and KIX9 (Figure S1a) (Gonzalez *et al.*, 2015).

Next to KIX8 and KIX9, nine other proteins that contain a KIX domain have been described in Arabidopsis (Thakur *et al.*, 2013). Beside their KIX domain, several KIX domain-containing proteins display additional similarities to non-plant KIX family members such as HISTONE ACETYLTRANFERASE (HAT) proteins and Mediator subunits (Kumar *et al.*, 2018; Thakur *et al.*, 2013). HAT proteins and Mediator subunits are known to function as co-activators through the interaction of their KIX domain with the transactivation domain of transcription factors (Kumar *et al.*, 2018; Thakur *et al.*, 2014). Except for their N-terminal KIX domain, however, KIX8 and KIX9 do not show any similarity to these co-activators (Thakur *et al.*, 2013). Instead, they hold an ETHYLENE RESPONSE FACTOR (ERF)-ASSOCIATED AMPHIPHILIC REPRESSION (EAR) motif that allows them to recruit the transcriptional co-repressor TOPLESS (TPL) (Causier *et al.*, 2012; Gonzalez *et al.*, 2015; Kagale *et al.*, 2010). In addition, they can simultaneously interact with the repressor PPD2 through their KIX domain (Gonzalez *et al.*, 2015). Hence, KIX8/KIX9 forms a molecular bridge between PPD2 and TPL (Figure S1a) and, because of that, PPD2 can act as a negative transcriptional regulator (Gonzalez *et al.*, 2015).

In Arabidopsis, the activity of the PPD/KIX repressor complex is regulated by the F-box protein STERILE APETALA (SAP) (Li *et al.*, 2018b; Wang *et al.*, 2016). Interaction of the repressor complex with SAP results in the proteasomal degradation of both KIX and PPD proteins (Figure S1a) (Li *et al.*, 2018b; Wang *et al.*, 2016). The KIX proteins seem to be required for the SAP-mediated proteasomal degradation of PPD1 and PPD2, but not the other way around (Li *et al.*, 2018b). In accordance with these observations, *SAP* overexpression plants produce enlarged rosettes composed of enlarged and dome-shaped leaves (Wang *et al.*, 2016).

Orthologs of the PPD, KIX, and SAP proteins were found in members of both eudicot and monocot species, but appear to be absent from Poaceae species (grasses), suggesting that the PPD-KIX-SAP module was lost in the grass lineage (Gonzalez *et al.*, 2015; Wang *et al.*, 2016). This might reflect the absence of self-renewing meristemoids in the stomatal lineage of grasses (Gonzalez *et al.*, 2015; Liu *et al.*, 2009; Vatén and Bergmann, 2012; Wang *et al.*, 2016). Several eudicot members, in which orthologs of the *PPD* or *KIX* genes were mutated or downregulated, including *Medicago truncatula*, soybean (*Glycine max*), blackgram (*Vigna mungo*), and pea (*Pisum sativum*), produced enlarged leaves (Ge *et al.*, 2016; Kanazashi *et al.*, 2018; Li *et al.*, 2019; Naito *et al.*, 2017). Moreover, overexpression of *SAP* orthologs in poplar (*Populus trichocarpa*) and cucumber (*Cucumis sativus* L.) also increased leaf size (Townsley *et al.*, 2015; Yang *et al.*, 2018; Yordanov *et al.*, 2017). The role of the PPD-KIX repressor complex in controlling leaf growth and its regulation by the F-box protein SAP, thus, seem to be conserved among distinct eudicot species. All of the aforementioned eudicots belong to the rosids though, which together with the asterids, constitute most of the core eudicot species (Figure S1b). Whether the orthologs of the PPD, KIX, and SAP proteins also function as regulators of leaf growth in asterid members has not been investigated yet.

Here, we report a conserved role for the KIX8 and KIX9 proteins in the regulation of leaf growth in tomato (*Solanum lycopersicum*), which is an asterid model species. We used protein interaction assays in yeast to demonstrate that the tomato orthologs of Arabidopsis KIX8 and KIX9 function as TPL adaptor proteins for the tomato PPD proteins. Next, we used CRISPR-Cas9 genome editing to simultaneously knockout the tomato *KIX8* and *KIX9* genes in the cultivar Micro-Tom. Double *kix8 kix9* tomato knockout lines produced enlarged, dome-shaped leaves and displayed increased expression of genes orthologous to Arabidopsis PPD2 target genes. Finally, we revealed that these *kix8 kix9* mutants carried larger fruits with increased pericarp thickness, which are important agronomic traits for fruit crops.

Results

Tomato KIX8 and KIX9 are conserved TPL adaptors for PPD proteins

To identify the tomato orthologs of the Arabidopsis KIX8 and KIX9 proteins, BLASTP was used. The tomato orthologs of the Arabidopsis PPD proteins have been described previously (Chini *et al.*, 2017). The tomato KIX and PPD proteins display a similar domain structure as their Arabidopsis counterparts (Figure S2). Amplification of the coding sequences of tomato *KIX* and *PPD* genes revealed alternative splicing for *KIX9*, *PPD1*, and *PPD2* (Figure S2b,c,d). Based on an alternative splicing model for Arabidopsis *KIX9* reported by The Arabidopsis Information Resource (TAIR), we hypothesized that retention of the second tomato *KIX9* intron leads to the use of a downstream start codon, generating a splice variant that lacks the N-terminal KIX domain (Figure S2b). The splice variants of *PPD1* and *PPD2* display retention of the Jas intron and part of the Jas intron, respectively, which is located between the two exons encoding the Jas domain (Figure S2c,d). These alternative splicing events are proposed to generate premature stop codons (Figure S2c,d), and consequently truncated PPD proteins, as was previously shown for Arabidopsis *PPD1* and *PPD2* (Li *et al.*, 2016).

To determine whether KIX8, KIX9, PPD1, and PPD2 are part of a protein complex similar to the Arabidopsis PPD2-KIX8/KIX9 complex, we performed yeast two-hybrid (Y2H) assays. For these assays, the proteins encoded by the first splice variants shown in Figure S2 were used. In case of the KIX proteins, these possessed the KIX domain assumed to be essential for interaction with the PPD proteins. Direct interaction between the KIX and PPD proteins could be observed (Figure 1a). Next, we evaluated whether the KIX proteins were able to interact with TPL1 (Figure 1b), which is the most closely related tomato ortholog of the Arabidopsis co-repressor TPL (Hao *et al.*, 2014). As only KIX8 was capable of interacting with TPL1 in the Y2H assays (Figure 1b), we also assessed the interaction between the KIX proteins and the five additional TPL proteins that were reported in tomato (Hao *et al.*, 2014) (Figure 1b). In addition to TPL1, KIX8 also interacted with TPL2, TPL4, and TPL6, whereas KIX9 could solely interact with TPL2 (Figure 1b). By means of yeast three-hybrid (Y3H) assays, we could show that the KIX proteins can form a molecular bridge between these TPL proteins and the PPD proteins (Figure 1c,d). In Arabidopsis, both the KIX and PPD proteins were reported to interact with the F-box protein SAP, resulting in their post-translational degradation (Li *et al.*, 2018b; Wang *et al.*, 2016). However, we only observed interaction between KIX8 and the tomato ortholog of Arabidopsis SAP (Figure 1e,f). Taken together, our results demonstrate that

in tomato, KIX8 and KIX9 function as TPL adaptors for the PPD proteins, similar to their orthologs in Arabidopsis.

CRISPR-Cas9 genome editing of tomato *KIX8* and *KIX9* leads to enlarged dome-shaped leaves

To investigate the *in planta* role of tomato KIX8 and KIX9, we generated double *kix8 kix9* loss-of-function mutants (cultivar Micro-Tom) using Clustered Regularly Interspaced Short Palindromic Repeats-CRISPR associated protein 9 (CRISPR-Cas9) genome editing (Figure 2a). A rippled, dome-shaped leaf phenotype could already be observed in regenerated double *kix8 kix9* knockout (T0) plants (Figure S3). Likewise, the progeny of two independent T1 plants mono- or biallelic for out-of-frame mutations at both the *KIX8* and *KIX9* loci (Figure S4a,b), displayed dome-shaped leaves with uneven leaf laminae (Figure 2b,c). Single *kix8* mutants (Figure S4a,b), obtained by pollinating the *kix8-kix9*$^{\#10}$ (T1) line with wild-type pollen, exhibited an intermediate leaf phenotype (Figure 2b,c), whereas single *kix9* plants (Figure S4a,b) did not show any visible phenotype (Figure 2b,c) as was noted for Arabidopsis *kix8* or *kix9* single mutants (Gonzalez *et al.*, 2015). These observations suggest that KIX8 and KIX9 may have partially redundant roles in regulating tomato leaf growth.

Given that the rippled, dome-shaped leaf phenotype was most pronounced for double *kix8 kix9* mutants, phenotypical analyses were performed on leaf eight and compared with measurements on the corresponding wild-type leaf. First, leaf fresh weight was determined, which was approximately 1.3-fold higher for *kix8 kix9* leaves compared with wild-type leaves (Figure 3a). Likewise, the fresh weight of the terminal leaflets of these *kix8 kix9* leaves was increased with approximately 40% compared with those of wild-type leaves (Figure 3b). Next, the area of terminal leaflets was measured before (projected area) and after (real area) terminal leaflets were cut to flatten them (Figure 3c,d) (Baekelandt *et al.*, 2018). After flattening the terminal leaflets, those of *kix8 kix9* mutants displayed an area that was approximately 1.4-fold larger than corresponding wild-type leaflets (Figure 3e). In addition, the decrease in projected-to-real terminal leaflet area was about two times bigger for *kix8-kix9* plants compared with wild-type plants (Figure 3f), demonstrating the alteration in *kix8 kix9* leaflet shape. These measurements, thus, substantiate the enlarged, dome-shaped leaf phenotype of double *kix8 kix9* knockout plants.

Putative PPD target genes are upregulated in leaves of tomato *kix8 kix9* mutants

To gain further insight into the function of KIX8 and KIX9 in tomato plants, we made use of public transcriptome data (cultivar Micro-Tom) (Zouine *et al.*, 2017) to investigated the gene expression patterns of *KIX8*, *KIX9*, *PPD1*, and *PPD2* in different tissues and throughout distinct developmental stages. A survey of these publicly available transcriptome data revealed that *KIX8* was lowly expressed in all examined tissues and that *KIX9* expression was (nearly) absent in most tissues (Figure 4a and Table S1). In all investigated tissues, the transcript level of *PPD2* was higher than that of *PPD1* (Figure 4a and Table S1). Next, we looked up the gene expression patterns of the putative tomato orthologs of Arabidopsis *DWARF IN LIGHT 1* (*DFL1*), *AT-HOOK MOTIF CONTAINING NUCLEAR LOCALISED PROTEIN 17* (*AHL17*), and *SCHLAFMUTZE* (*SMZ*), which were top-ranked in the list of differentially expressed genes in Arabidopsis *ami-ppd* leaves and strongly upregulated in Arabidopsis *kix8 kix9* leaves (Gonzalez *et al.*, 2015). Expression of all three tomato genes, *DFL1*, *AHL17*, and *APETALA 2d* (*AP2d*), was confirmed in tomato leaves (Figure 4b and Table S1). To verify the potential differential expression of these genes in tomato *kix8 kix9* mutants, we performed a quantitative real-time PCR (qPCR) analysis on the terminal leaflet of not fully developed leaves and found that the transcription of all three genes was higher in *kix8 kix9* mutants than in wild-type (Figure 4c). Furthermore, the expression of *KIX8* and *KIX9* was increased in *kix8 kix9* plants compared with wild-type plants (Figure 4d), suggesting negative feedback of the PPD-KIX complex on the expression of *KIX8* and *KIX9*. We conclude that KIX8 and KIX9 are required for the repression of tomato genes orthologous to three Arabidopsis PPD2 target genes (*DFL1*, *AHL17*, and *SMZ*) and, thereby, for the regulation of tomato leaf growth.

Tomato *kix8 kix9* mutants produce bigger tomato fruits

In multiple eudicot species that belong to the rosid order of Fabales, orthologs of the KIX and PPD proteins have been reported to negatively regulate seed pod size (Ge *et al.*, 2016; Kanazashi *et al.*, 2018; Li *et al.*, 2019; Naito *et al.*, 2017). To examine whether the KIX proteins might also have a role in determining tomato fruit size in the asterid model species tomato, we investigated whether the development of reproductive organs was affected in tomato *kix8 kix9* mutants. While growing the *kix8 kix9* mutants, we noted that they displayed a significant delay in flowering compared with wild-type plants (Figure 5a). In addition, though seed size and number were not altered (Figure S5a,b), we did observe an increase in *kix8 kix9* fruit size compared with wild-type fruits (Figure 5b). The fresh weight of tomatoes produced by *kix8 kix9*

plants was increased with approximately 80% compared with those produced by wild-type plants (Figure 5c). Accordingly, the diameter of *kix8 kix9* fruits was approximately 1.2-fold larger than that of wild-type fruits (Figure 5d). Cutting along the equatorial plane revealed that fruits from *kix8 kix9* mutants displayed an approximate increase of 1.7-fold in pericarp thickness compared with wild-type fruits (Figure 6a,b). Altogether, these data demonstrate that knocking out *KIX8* and *KIX9* in tomato results in the production of enlarged fruits, a favorable agronomic trait, and suggest that KIX8 and KIX9 are involved in the regulation of tomato fruit growth.

Discussion

KIX8 and KIX9 are conserved regulators of leaf growth in distinct eudicot species

In Arabidopsis, the asymmetric cell division of meristemoids, which are precursor cells of the stomatal lineage, positively affects final leaf size and is restricted by a transcriptional repressor complex in which the co-repressor TPL is recruited to PPD2 by KIX8/KIX9 (Gonzalez *et al.*, 2015; White, 2006). Members of this repressor complex were shown to regulate leaf size and shape in a variety of species that belong to different orders of the rosids (Ge *et al.*, 2016; Gonzalez *et al.*, 2015; Kanazashi *et al.*, 2018; Li *et al.*, 2019; Naito *et al.*, 2017), suggesting that the repressor complex is a conserved regulator of leaf growth among rosid eudicots. Here, we demonstrate that the tomato orthologs of KIX8 and KIX9 act as TPL adaptors for PPD proteins as well and, thereby, regulate leaf growth in tomato, a model species of the asterid clade that also includes tobacco (*Nicotiana tabacum*), carrot (*Daucus carota*) and sunflower (*Helianthus annuus*). In the rosid species Arabidopsis and pea, the interaction between KIX and PPD proteins is described to occur through the N-terminal KIX and PPD domain, respectively (Gonzalez *et al.*, 2015; Li *et al.*, 2019). This is likely to be the case in tomato as well, in which the KIX and PPD proteins display a similar domain structure. The interaction between tomato KIX8/KIX9 and the TPL co-repressors is expected to occur via the EAR motif present in the KIX proteins (Causier *et al.*, 2012; Kagale *et al.*, 2010), as was shown for their Arabidopsis and pea orthologs (Gonzalez *et al.*, 2015; Li *et al.*, 2019).

Overexpression of Arabidopsis *SAP* and its orthologs in several eudicot species was reported to increase leaf size (Wang *et al.*, 2016; Yang *et al.*, 2018; Yordanov *et al.*, 2017). Both the PPD and KIX proteins were suggested to be subject to proteasomal degradation in Arabidopsis through their interaction with SAP (Li *et al.*, 2018b; Wang *et al.*, 2016). Direct binding to the F-box protein SAP was, however, only reported for the KIX proteins and not for

the PPD proteins (Li *et al.*, 2018b; Wang *et al.*, 2016). Likewise, we only observed interaction between the tomato orthologs of SAP and KIX8 in yeast cells. Moreover, SAP-mediated degradation of the PPD proteins in Arabidopsis depends on the KIX proteins but not vice versa (Li *et al.*, 2018b). These observations highlight the importance of KIX8 and KIX9 for the regulation of eudicot leaf growth by the PPD proteins.

Tomato *kix8 kix9* plants exhibited an enlarged, dome-shaped leaf phenotype, similar to the one observed in Arabidopsis *ami-ppd* and *kix8 kix9* mutants (Gonzalez *et al.*, 2015). Moreover, terminal leaflets of young tomato *kix8 kix9* leaves displayed an increased expression of three putative PPD target genes, *DFL1*, *AHL17*, and *AP2d*, of which the orthologs were strongly upregulated in Arabidopsis *ami-ppd* and *kix8 kix9* leaves (Gonzalez *et al.*, 2015). Therefore, the tomato PPD-KIX complex might restrict meristemoid division, as shown in Arabidopsis (Gonzalez *et al.*, 2015; White, 2006), to control leaf development. Following the fate of meristemoids in tomato *kix8 kix9* leaves over time could help us validate this. Taken together, we can conclude that both in asterid and rosid species, KIX8 and KIX9 assist PPD proteins in repressing distinct downstream target genes to regulate leaf size and shape.

Partial redundancy of KIX8 and KIX9

The KIX8 and KIX9 proteins were reported to have partially redundant roles in controlling Arabidopsis leaf growth (Gonzalez *et al.*, 2015). The intermediate and absent leaf phenotype of tomato single *kix8* and *kix9* mutants, respectively, compared with the markedly enlarged, dome-shaped leaf phenotype of tomato *kix8 kix9* plants, suggests partial redundancy of KIX8 and KIX9 in tomato leaf development as well. In line with these phenotypes, transcription of *KIX9* is (nearly) absent in most tomato tissues, whereas *KIX8* displays higher expression. In tomato *kix8 kix9* tomato leaflets, however, the transcript levels of not only *KIX8* but also *KIX9* were increased compared with wild-type leaflets, suggesting negative feedback of the PPD-KIX complex on the expression of both *KIX8* and *KIX9*. In yeast cells, interaction with TPL2 was observed for both KIX8 and KIX9, but KIX8 could additionally interact with TPL1, TPL4, TPL6, and SAP. A previous study showed that from the six tomato TPL genes, *TPL1* had the highest overall expression in examined tissues and developmental stages, while *TPL2* was expressed to a much lesser extent (Hao *et al.*, 2014). The expression of *TPL4* dominated in ripening fruit and *TPL6* transcripts were nearly absent in all investigated tissues (Hao *et al.*, 2014). Furthermore, TPL6 was suggested to have lost its functionality (Hao *et al.*, 2014) and, therefore, calls the biological relevance of the interaction between KIX8 and TPL6 into question. To further explore this, it could be relevant to investigate the tissue-specific

interactions between KIX and TPL proteins *in planta*. All in all, these data indicate that KIX8 and KIX9 are functionally redundant, but that KIX8 might play a predominant role in the regulation of leaf development.

KIX8 and KIX9 are negative regulators of fruit growth

Like any other plant organ, fruit grows by means of cell division and cell expansion. After fertilization, tomato ovary growth starts by a short period of cell proliferation followed by a longer cell expansion phase, resulting in a massive expansion of the pericarp (or fruit flesh) in particular (Xiao *et al.*, 2009). Fruit ripening commences after fruit growth is finalized. Here, we report that simultaneously knocking out *KIX8* and *KIX9* by CRISRP-Cas9 genome editing results in the production of bigger tomato fruits with increased pericarp thickness. Whether this is the consequence of prolonged cell division or cell expansion, or a combination of both still needs to be investigated and could provide hints for putative target genes.

In line with our findings, several rosid eudicot species, in which the *KIX* or *PPD* genes were either mutated or downregulated, displayed increased seed (pod) size (Ge *et al.*, 2016; Li *et al.*, 2018a). Furthermore, orthologs of Arabidopsis *SAP*, which encodes an F-box protein that regulates the stability of the PPD-KIX complex, are positive regulators of fruit and flower size in cucumber and of flower size in *Capsella rubella* (Sicard *et al.*, 2016; Yang *et al.*, 2018). Therefore, it is likely that also target genes involved in tomato fruit growth are regulated by the PPD-KIX repressor complex. Taken together, these observations indicate that KIX8 and KIX9 are negative regulators of fruit size, which was among the main selection criteria for nearly all fruit crops during domestication and still is today (Pickersgill, 2007).

Experimental procedures

Ortholog identification

Tomato orthologs of *A. thaliana* KIX8 and KIX9 were identified through a BLASTP search in the National Center for Biotechnology Information (NCBI) GenBank protein database. Tomato orthologs of *A. thaliana* SAP, DFL1, AHL17, and SMZ were retrieved from the comparative genomics resource PLAZA 4.0 Dicots (http://bioinformatics.psb.ugent.be/plaza/) (Van Bel *et al.*, 2018).

DNA Constructs

Yeast two- and three-hybrid constructs

For yeast two- (Y2H) and three-hybrid (Y3H) assays, the coding sequence of tomato *KIX8*, *KIX9*, *PPD1*, *PPD2*, and *SAP* was PCR-amplified with the primers listed in Table S2 and recombined in a Gateway donor vector (Invitrogen). Gateway donor vectors containing the coding sequence of tomato *TPL1–6* were obtained from (Hao *et al.*, 2014). Subsequently, Gateway LR reactions (Invitrogen) were performed with pGAD424gate and pGBT9gate, generating bait and prey constructs, respectively. Alternatively, MultiSite Gateway LR reactions (Invitrogen) were performed with pMG426 (Nagels Durand *et al.*, 2012) to express a third protein of interest, driven by the *GDP* promoter and C-terminally fused to the SV40 NLS-3xFLAG-6xHis tag.

CRISPR-Cas9 constructs

To select CRISPR-Cas9 guide (g)RNA target sites, CRISPR-P (http://crispr.hzau.edu.cn/CRISPR/) (Lei *et al.*, 2014) was used. We selected a gRNA target site in the first exon of *KIX8*, whereas for *KIX9*, we selected a gRNA target site in the third exon downstream of a start codon that could act as an alternative transcription start site (Figure S2b). The CRISPR-Cas9 construct was cloned as previously described (Fauser *et al.*, 2014; Pauwels *et al.*, 2018; Ritter *et al.*, 2017). Briefly, for each gRNA target site, two complementary oligonucleotides with 4-bp overhangs (Table S2) were annealed and inserted by a Golden Gate reaction with *Bpi*I (Thermo Scientific) and T4 DNA ligase (Thermo Scientific) in a Gateway entry vector. As Gateway entry vectors, pMR217 (L1-R5) and pMR218 (L5-L2) (Ritter *et al.*, 2017) were used. Next, a MultiSite Gateway LR reaction (Invitrogen) was used to recombine two gRNA modules with pDe-Cas9-Km (Ritter *et al.*, 2017).

Yeast two- and three-hybrid assays

Y2H and Y3H assays were performed as described previously (Cuéllar Pérez *et al.*, 2013). Briefly, for Y2H assays, the *Saccharomyces cerevisiae* PJ69-4A yeast strain was co-transformed with bait and prey constructs using the polyethylene glycol (PEG)/lithium acetate method. Transformants were selected on Synthetic Defined (SD) medium lacking Leu and Trp (−2) (Clontech). Three individual transformants were grown overnight in liquid SD (−2) medium and 10-fold dilutions of these cultures were dropped on SD control (−2) and selective medium additionally lacking His (−3) (Clontech). Empty vectors were used as negative controls. Yeast plates were allowed to grow for 2 days at 30°C before interaction was scored. Y3H assays were performed in the same way, but with different SD media compositions. For transformant selection and culturing in control media, SD medium lacking Leu, Trp, and Ura (−3) was used, while selective media additionally lacked His (−4) (Clontech).

Plant material and growth conditions

S. lycopersicum (cultivar Micro-Tom) and CRISPR-Cas9 mutant seeds were sown in soil. Plants were grown under long-day photoperiods (16:8). Daytime and nighttime temperatures were 26–29°C and 18–20°C, respectively.

Tomato plant transformation

Binary constructs were introduced in competent *Agrobacterium tumefaciens* (strain EHA105) cells using electroporation and transformed into *S. lycopersicum* (cultivar Micro-Tom) using the cotyledon transformation method as reported previously (Gonzalez *et al.*, 2007) with following modifications. Cotyledon pieces from one-week-old seedlings were incubated for 24 h in de dark at 25°C on solid Murashige and Skoog (MS) medium (pH 5.7) containing 4.4 g/L of MS supplemented with vitamins (Duchefa), 20 g/L of sucrose, 0.2 g/L of KH_2PO_4, 1 mg/L thiamine, 0.2 mM acetosyringone, 0.2 mg/L 2,4-dichlorophenoxyacetic acid (2,4-D), and 0.1 mg/L kinetin. Next, the cotyledon pieces were soaked in a *A. tumefaciens* (strain EHA105) bacterial suspension culture (0.05-0.10 OD) containing the binary vector for 25 min with shaking. Cotyledon pieces were dried on sterile tissue paper and placed back on the aforementioned solid MS medium for 48 h in the dark at 25°C. Cotyledon pieces were washed once with liquid MS medium (pH 5.7) containing 4.4 g/L of MS supplemented with vitamins (Duchefa), containing 20 g/L of sucrose, 0.2 g/L of KH_2PO_4, and 1 mg/L thiamine and once with sterile water. Cotyledon pieces were dried on sterile tissue paper and placed on solid MS

medium (pH 5.7) containing 4.4 g/L of MS supplemented with vitamins (Duchefa), containing 30 g/L of sucrose, 1 mL/L 1000X Nitsch vitamin stock (for 100 mL: 0.005 g biotin, 0.2 g glycine, 10 g myo-inositol, 0.5 g nicotinic acid, 0.05 g pyridoxine HCl, and 0.05 g thiamine HCl), 0.5 g/L folic acid, 2 mg/L zeatin riboside, 100 mg/L kanamycin, 25 mg/L melatonin, and 300 mg/L timentin and put in a 25°C controlled photoperiodic growth chamber (16:8 photoperiods). The aforementioned medium was changed every 14 days until regenerated shoots appeared. These shoots were placed on solid MS medium (pH 5.7) containing 2.2 g/L of MS, 10 g/L of sucrose, 1 mL/L 1000X Nitsch vitamin stock, 0.5 g/L folic acid, 100 mg/L kanamycin, and 150 mg/L timentin until their acclimatization in the greenhouse.

Identification of CRISPR-Cas9 mutants

Plant genotyping

CRISPR-Cas9 mutants were identified as described previously (Swinnen *et al.*, 2020). Genomic DNA was prepared from homogenized leaf tissue using extraction buffer (pH 9.5) containing 0.1 M of tris(hydroxymethyl)aminomethane (Tris)-HCl, 0.25 M of KCl, and 0.01 M of ethylenediaminetetraacetic acid (EDTA). The mixture was incubated at 95°C for 10 min and cooled at 4°C for 5 min. After addition of 3% (w/v) BSA, collected supernatant was used as a template in a standard PCR reaction using GoTaq (Promega) with Cas9-specific primers (to select primary plant transformant (T0) lines in which the T-DNA was present or plant T1 lines in which the T-DNA was absent) or with primers to amplify a gRNA target region (Table S2). PCR amplicons containing a gRNA target site were purified using HighPrep PCR reagent (MAGBIO). After Sanger sequencing of the purified PCR amplicons with an amplification primer located approximately 200 bp from the Cas9 cleavage site, quantitative sequence trace data were decomposed using Tracking Indels by DEcomposition (TIDE) (https://www.deskgen.com/landing/tide.html#/tide) or Inference of CRISPR Editing (ICE) Analysis Tool (https://ice.synthego.com/#/).

Plant ploidy level analysis

Diploid CRISPR-Cas mutants (T0) were identified using flow cytometry. Leaf material (1.0 cm^2) was chopped in 200 µL of chilled CyStain UV Precise P Nuclei Extraction Buffer (Sysmex) for 2 min using a razor blade. The suspension was filtered through a 50-µm nylon filter and 800 µL of chilled CyStain UV Precise P Staining Buffer (Sysmex) was added to the

isolated nuclei. The DNA content of 5,000–10,000 nuclei was measured using a CyFlow Space flow cytometer (Sysmex) and analyzed with FloMax software (Sysmex).

Phenotypic analyses

Leaf growth parameter analysis

The eighth leaf (from the top) from 2–month–old CRISPR-Cas mutant (T2) and wild-type plants was harvested for leaf growth parameter analysis. Per genotype, 31–40 biological replicates (leaves) were collected. A digital balance was used to measure the biomass/fresh weight of leaves and their terminal leaflets. Pictures of terminal leaflets were taken before (projected) and after (real) cutting the leaves to flatten them. Projected and real leaflet area were measured using ImageJ (https://imagej.nih.gov/ij/). Statistical significance was determined by ANOVA followed by Tukey post-hoc analysis ($P < 0.05$).

Flowering time analysis

Flowering time of CRISPR-Cas mutant (T2) and wild-type plants was quantified by counting the number of true leaves that were produced before initiation of the primary inflorescence (Soyk *et al.*, 2017). Flowering time was measured for 15–16 plants per genotype. Statistical significance was determined by ANOVA followed by Tukey post-hoc analysis ($P < 0.05$).

Fruit growth parameter analysis

For fruit size and biomass measurements, red ripe fruits from CRISPR-Cas mutant (T2) and wild-type plants were harvested. Per genotype, 20–36 biological replicates (individual fruits) were collected. Fruit size was determined by measuring the maximum diameter of the equatorial fruit axis. To determine fruit pericarp thickness, fruits in breaker–orange (breaker + 3 days) stage were harvested and scans were taken of the equatorial sections. Per genotype, 18–20 biological replicates (individual fruits) were collected. Pericarp thickness was measured using Tomato Analyzer (version 4.0) (Brewer *et al.*, 2006). Statistical significance was determined by ANOVA followed by Tukey post-hoc analysis ($P < 0.05$).

Seed parameter analysis

For seed size and number analyses, seeds were harvested from red ripe fruits produced by CRISPR-Cas mutant (T2) and wild-type plants. Per genotype, 20–36 biological replicates

(fruits) were collected. Statistical significance was determined by ANOVA followed by Tukey post-hoc analysis ($P < 0.05$).

Gene expression analysis by quantitative real-time PCR

The terminal leaflet of the second leaf (from the top) from 3-week-old CRISPR-Cas mutant (T2) and wild-type plants was harvested by flash freezing in liquid nitrogen and ground using the Mixer Mill 300 (Retch). Per genotype, five biological replicates that each consisted of a single terminal leaflet were collected. Messenger RNA was extracted from homogenized tissue as described in (Townsley *et al.*, 2015) with following modifications. Tissue was lysed using 800 µL of lysate binding buffer (LBB) containing 100 mM of Tris-HCl (pH 7.5), 500 mM of LiCl, 10 mM of EDTA (pH 8.0), 1% of sodium dodecyl sulfate (SDS), 5 mM of dithiothreitol (DTT), 15 µL/mL of Antifoam A, and 5 µL/mL of 2-mercaptoethanol, and the mixture was incubated for 10 min at room temperature. Messenger RNA was separated from 200 µL of lysate using 1 µL of 12.5 µM of 5' biotinylated polyT oligonucleotide (5'-biotin-ACAGGACATTCGTCGCTTCCTTTTTTTTTTTTTTTTT-3') and the mixture was incubated for 10 min. Next, captured messenger RNA was isolated from the lysate by adding 20 µL LBB-washed streptavidin-coated magnetic beads (New England Biolabs) and was allowed to stand for 10 min at room temperature. Samples were placed on a MagWell Magnetic Separator 96 (EdgeBio) and washed with 200 µL of washing buffer A (10 mM of Tris-HCl (pH 7.5), 150 mM of LiCl, 1 mM of EDTA (pH 8.0), 0.1% of SDS), washing buffer B (10 mM of Tris-HCl (pH 7.5), 150 mM of LiCl, 1 mM of EDTA (pH 8.0)), and low-salt buffer (20 mM of Tris-HCl (pH 7.5), 150 mM of NaCl, 1 mM of EDTA (pH 8.0)), all pre-chilled on ice. Elution of messenger RNA was done by adding 20 µL of 10 mM of Tris-HCl (pH 8.0) with 1 mM of 2-mercaptoethanol followed by incubation of the mixture at 80°C for 2 min.

First-strand complementary DNA was synthesized from 20 µL of messenger RNA eluate by qScript cDNA Synthesis Kit (Quantabio). Quantitative real-time PCR (qPCR) reactions were carried out with a LightCycler 480 System (Roche) using Fast SYBR Green Master Mix (Applied Biosystems) and primers (Table S2) designed by QuantPrime (https://www.quantprime.de/) (Arvidsson *et al.*, 2008). Gene expression levels were quantified relative to *CLATHRIN ADAPTOR COMPLEXES MEDIUM SUBUNIT* (*CAC*) and *TAP42-INTERACTING PROTEIN* (*TIP41*) using the $2^{-\Delta\Delta Ct}$ method (Livak and Schmittgen, 2001). Statistical significance was determined by ANOVA followed by Tukey post-hoc analysis ($P < 0.05$).

Accession numbers

Sequence data from this article can be found in the EMBL/GenBank/Solgenomics data libraries under the following accession numbers: *KIX8* (Solyc07g008100), *KIX9* (Solyc08g059700), *PPD1* (Solyc06g084120), *PPD2* (Solyc09g065630), *SAP* (Solyc05g041220), *DFL1* (Solyc07g063850), *AHL17* (Solyc04g076220), *AP2d* (Solyc11g072600), *CAC* (Solyc08g006960), and *TIP41* (Solyc10g049850).

Author contributions

G.S., A.B., L.P., and A.G. designed the experiments. G.S., A.B., R.D.C., J.V.D., and N.G. performed the experiments. G.S., A.B., L.P., A.G., and D.I. analyzed the data. G.S. wrote the article and A.B., L.P., A.G. and N.G. complemented the writing.

Acknowledgements

This work was supported by the Research Foundation Flanders (FWO) through the projects G005312N, G004515N, and 3G038719 and a postdoctoral fellowship to L.P. We thank Annick Bleys for help with preparing the manuscript and Mohamed Zouine for sharing plasmids containing the coding sequence of tomato *TPL1–6* with us.

Supporting information

Additional supporting information may be found online in the Supporting Information section at the end of the article.

Figure S1 A conserved repressor complex regulates leaf growth in distinct eudicot species.
Figure S2 Splice variants of tomato *KIX8*, *KIX9*, *PPD1*, and *PPD2*.
Figure S3 Regenerated tomato *kix8 kix9* plants display a rippled, dome-shaped leaf phenotype.
Figure S4 CRISPR-Cas9 mutations in tomato double *kix8 kix9* (T1), single *kix8*, and *kix9* knockout lines.
Figure S5 Tomato *kix8 kix9* plants do not exhibit a seed phenotype.
Table S1 Normalized expression of *KIX8*, *KIX9*, *PPD1*, *PPD2*, *DFL1*, *AHL17,* and *AP2d* in different tomato organs and developmental stages (cultivar Micro-Tom) used to draw heat maps in Figure 4a–b.
Table S2 Oligonucleotides used in this study.

References

Arvidsson, S., Kwasniewski, M., Riaño-Pachón, D.M. and Mueller-Roeber, B. (2008) QuantPrime - a flexible tool for reliable high-throughput primer design for quantitative PCR. *BMC Bioinformatics* **9**, 465.

Baekelandt, A., Pauwels, L., Wang, Z.B., Li, N., De Milde, L., Natran, A., Vermeersch, M., Li, Y., Goossens, A., Inzé, D. and Gonzalez, N. (2018) Arabidopsis leaf flatness is regulated by PPD2 and NINJA through repression of *CYCLIN D3* genes. *Plant Physiology* **178**, 217-232.

Bai, Y., Meng, Y., Huang, D., Qi, Y. and Chen, M. (2011) Origin and evolutionary analysis of the plant-specific TIFY transcription factor family. *Genomics* **98**, 128-136.

Brewer, M.T., Lang, L., Fujimura, K., Dujmovic, N., Gray, S. and van der Knaap, E. (2006) Development of a controlled vocabulary and software application to analyze fruit shape variation in tomato and other plant species. *Plant Physiology* **141**, 15-25.

Causier, B., Ashworth, M., Guo, W. and Davies, B. (2012) The TOPLESS interactome: a framework for gene repression in Arabidopsis. *Plant Physiology* **158**, 423-438.

Chini, A., Ben-Romdhane, W., Hassairi, A. and Aboul-Soud, M.A.M. (2017) Identification of TIFY/JAZ family genes in *Solanum lycopersicum* and their regulation in response to abiotic stresses. *Plos One* **12**, e0177381.

Chini, A., Fonseca, S., Chico, J.M., Fernández-Calvo, P. and Solano, R. (2009) The ZIM domain mediates homo- and heteromeric interactions between Arabidopsis JAZ proteins. *Plant Journal* **59**, 77-87.

Chini, A., Fonseca, S., Fernández, G., Adie, B., Chico, J.M., Lorenzo, O., García-Casado, G., López-Vidriero, I., Lozano, F.M., Ponce, M.R., Micol, J.L. and Solano, R. (2007) The JAZ family of repressors is the missing link in jasmonate signalling. *Nature* **448**, 666-671.

Chung, H.S. and Howe, G.A. (2009) A critical role for the TIFY motif in repression of jasmonate signaling by a stabilized splice variant of the JASMONATE ZIM-domain protein JAZ10 in *Arabidopsis*. *Plant Cell* **21**, 131-145.

Cuéllar Pérez, A., Pauwels, L., De Clercq, R. and Goossens, A. (2013) Yeast two-hybrid analysis of jasmonate signaling proteins. *Methods in Molecular Biology* **1011**, 173-185.

Fauser, F., Schiml, S. and Puchta, H. (2014) Both CRISPR/Cas-based nucleases and nickases can be used efficiently for genome engineering in *Arabidopsis thaliana*. *Plant Journal* **79**, 348-359.

Ge, L., Yu, J., Wang, H., Luth, D., Bai, G., Wang, K. and Chen, R. (2016) Increasing seed size and quality by manipulating *BIG SEEDS1* in legume species. *Proceedings of the National Academy of Sciences of the United States of America* **113**, 12414-12419.

Gonzalez, N., Gévaudant, F., Hernould, M., Chevalier, C. and Mouras, A. (2007) The cell cycle-associated protein kinase WEE1 regulates cell size in relation to endoreduplication in developing tomato fruit. *Plant Journal* **51**, 642-655.

Gonzalez, N., Pauwels, L., Baekelandt, A., De Milde, L., Van Leene, J., Besbrugge, N., Heyndrickx, K.S., Cuéllar Pérez, A., Nagels Durand, A., De Clercq, R., Van De Slijke, E., Vanden Bossche, R., Eeckhout, D., Gevaert, K., Vandepoele, K., De Jaeger, G., Goossens, A. and Inzé, D. (2015) A repressor protein complex regulates leaf growth in Arabidopsis. *Plant Cell* **27**, 2273-2287.

Gonzalez, N., Vanhaeren, H. and Inzé, D. (2012) Leaf size control: complex coordination of cell division and expansion. *Trends in Plant Science* **17**, 332-340.

Hao, Y., Wang, X., Li, X., Bassa, C., Mila, I., Audran, C., Maza, E., Li, Z., Bouzayen, M., van der Rest, B. and Zouine, M. (2014) Genome-wide identification, phylogenetic analysis, expression profiling, and protein–protein interaction properties of *TOPLESS* gene family members in tomato. *Journal of experimental botany* **65**, 1013-1023.

Hepworth, J. and Lenhard, M. (2014) Regulation of plant lateral-organ growth by modulating cell number and size. *Current Opinion in Plant Biology* **17**, 36-42.

Kagale, S., Links, M.G. and Rozwadowski, K. (2010) Genome-wide analysis of ethylene-responsive element binding factor-associated amphiphilic repression motif-containing transcriptional regulators in Arabidopsis. *Plant Physiology* **152**, 1109-1134.

Kalve, S., De Vos, D. and Beemster, G.T.S. (2014) Leaf development: a cellular perspective. *Frontiers in Plant Science* **5**, 362.

Kanazashi, Y., Hirose, A., Takahashi, I., Mikami, M., Endo, M., Hirose, S., Toki, S., Kaga, A., Naito, K., Ishimoto, M., Abe, J. and Yamada, T. (2018) Simultaneous site-directed mutagenesis of duplicated loci in soybean using a single guide RNA. *Plant Cell Reports*, in press (10.1007/s00299-018-2251-3).

Kumar, V., Waseem, M., Dwivedi, N., Maji, S., Kumar, A. and Thakur, J.K. (2018) KIX domain of AtMed15a, a Mediator subunit of Arabidopsis, is required for its interaction with different proteins. *Plant signaling & behavior* **13**, e1428514.

Lei, Y., Lu, L., Liu, H.-Y., Li, S., Xing, F. and Chen, L.-L. (2014) CRISPR-P: a web tool for synthetic single-guide RNA design of CRISPR-system in plants. *Molecular Plant* **7**, 1494-1496.

Li, C., Zong, Y., Wang, Y., Jin, S., Zhang, D., Song, Q., Zhang, R. and Gao, C. (2018a) Expanded base editing in rice and wheat using a Cas9-adenosine deaminase fusion. *Genome Biology* **19**, 59.

Li, N., Liu, Z., Wang, Z., Ru, L., Gonzalez, N., Baekelandt, A., Pauwels, L., Goossens, A., Xu, R., Zu, Z., Inzé, D. and Li, Y. (2018b) STERILE APETALA modulates the stability of a repressor protein complex to control organ size in *Arabidopsis thaliana*. *PLoS Genetics* **14**, e1007218.

Li, S., Yamada, M., Hang, X., Ohler, U. and Benfey, P.N. (2016) High-resolution expression map of the *Arabidopsis* root reveals alternative splicing and lincRNA regulation. *Developmental Cell* **39**, 508-522.

Li, X., Liu, W., Zhuang, L., Zhu, Y., Wang, F., Chen, T., Yang, J., Ambrose, M., Hu, Z., Weller, J.L. and Luo, D. (2019) BIGGER ORGANS and ELEPHANT EAR-LIKE LEAF1 control organ size and floral organ internal asymmetry in pea. *Journal of Experimental Botany* **70**, 179-191.

Liu, T., Ohashi-Ito, K. and Bergmann, D.C. (2009) Orthologs of *Arabidopsis thaliana* stomatal bHLH genes and regulation of stomatal development in grasses. *Development* **136**, 2265-2276.

Livak, K.J. and Schmittgen, T.D. (2001) Analysis of relative gene expression data using real-time quantitative PCR and the $2^{-\Delta\Delta CT}$ method. *Methods* **25**, 402-408.

Nagels Durand, A., Moses, T., De Clercq, R., Goossens, A. and Pauwels, L. (2012) A MultiSite Gateway™ vector set for the functional analysis of genes in the model *Saccharomyces cerevisiae*. *BMC Molecular Biology* **13**, 30.

Naito, K., Takahashi, Y., Chaitieng, B., Hirano, K., Kaga, A., Takagi, K., Ogiso-Tanaka, E., Thavarasook, C., Ishimoto, M. and Tomooka, N. (2017) Multiple organ gigantism caused by mutation in *VmPPD* gene in blackgram (*Vigna mungo*). *Breeding Science* **67**, 151-158.

Pauwels, L., Barbero, G.F., Geerinck, J., Tilleman, S., Grunewald, W., Cuéllar Pérez, A., Chico, J.M., Vanden Bossche, R., Sewell, J., Gil, E., García-Casado, G., Witters, E., Inzé, D., Long, J.A., De Jaeger, G., Solano, R. and Goossens, A. (2010) NINJA connects the co-repressor TOPLESS to jasmonate signalling. *Nature* **464**, 788-791.

Pauwels, L., De Clercq, R., Goossens, J., Iñigo, S., Williams, C., Ron, M., Britt, A. and Goossens, A. (2018) A dual sgRNA approach for functional genomics in *Arabidopsis thaliana*. *G3: Genes, Genomes, Genetics* **8**, 2603-2615.

Pickersgill, B. (2007) Domestication of plants in the Americas: insights from mendelian and molecular genetics. *Annals of Botany* **100**, 925-940.

Ritter, A., Iñigo, S., Fernández-Calvo, P., Heyndrickx, K.S., Dhondt, S., Shi, H., De Milde, L., Vanden Bossche, R., De Clercq, R., Eeckhout, D., Ron, M., Somers, D.E., Inzé, D., Gevaert, K., De Jaeger, G., Vandepoele, K., Pauwels, L. and Goossens, A. (2017) The transcriptional repressor complex FRS7-FRS12 regulates flowering time and growth in *Arabidopsis*. *Nature communications* **8**, 15235.

Sicard, A., Kappel, C., Lee, Y.W., Woźniak, N. J., Marona, C., Stinchcombe, J.R., Wright, S.I. and Lenhard, M. (2016) Standing genetic variation in a tissue-specific enhancer underlies selfing-syndrome evolution in *Capsella*. *Proceedings of the National Academy of Sciences of the United States of America* **113**, 13911-13916.

Soyk, S., Müller, N.A., Park, S.J., Schmalenbach, I., Jiang, K., Hayama, R., Zhang, L., Van Eck, J., Jiménez-Gómez, J.M. and Lippman, Z.B. (2017) Variation in the flowering gene *SELF PRUNING 5G* promotes day-neutrality and early yield in tomato. *Nature Genetics* **49**, 162-168.

Swinnen, G., Jacobs, T., Pauwels, L. and Goossens, A. (2020) CRISPR-Cas-mediated gene knockout in tomato. *Methods in Molecular Biology* **2083**, 321-341.

Thakur, J.K., Agarwal, P., Parida, S., Bajaj, D. and Pasrija, R. (2013) Sequence and expression analyses of KIX domain proteins suggest their importance in seed development and determination of

seed size in rice, and genome stability in Arabidopsis. *Molecular Genetics and Genomics* **288**, 329-346.

Thakur, J.K., Yadav, A. and Yadav, G. (2014) Molecular recognition by the KIX domain and its role in gene regulation. *Nucleic Acids Research* **42**, 2112-2125.

Thines, B., Katsir, L., Melotto, M., Niu, Y., Mandaokar, A., Liu, G., Nomura, K., He, S.Y., Howe, G.A. and Browse, J. (2007) JAZ repressor proteins are targets of the SCF^{COI1} complex during jasmonate signalling. *Nature* **448**, 661-665.

Townsley, B.T., Covington, M.F., Ichihashi, Y., Zumstein, K. and Sinha, N.R. (2015) BrAD-seq: Breath Adapter Directional sequencing: a streamlined, ultra-simple and fast library preparation protocol for strand specific mRNA library construction. *Frontiers in Plant Science* **6**, 366.

Van Bel, M., Diels, T., Vancaester, E., Kreft, L., Botzki, A., Van de Peer, Y., Coppens, F. and Vandepoele, K. (2018) PLAZA 4.0: an integrative resource for functional, evolutionary and comparative plant genomics. *Nucleic Acids Research* **46**, D1190-D1196.

Vanholme, B., Grunewald, W., Bateman, A., Kohchi, T. and Gheysen, G. (2007) The tify family previously known as ZIM. *Trends in Plant Science* **12**, 239-244.

Vatén, A. and Bergmann, D.C. (2012) Mechanisms of stomatal development: an evolutionary view. *EvoDevo* **3**, 11.

Vercruysse, J., Baekelandt, A., Gonzalez, N. and Inzé, D. (2020) Molecular networks regulating the cell division during leaf growth in Arabidopsis. *Journal of experimental botany*, in press (10.1093/jxb/erz522).

Wang, Z., Li, N., Jiang, S., Gonzalez, N., Huang, X., Wang, Y., Inzé, D. and Li, Y. (2016) SCF^{SAP} controls organ size by targeting PPD proteins for degradation in *Arabidopsis thaliana*. *Nature communications* **7**, 11192.

White, D.W.R. (2006) *PEAPOD* regulates lamina size and curvature in *Arabidopsis*. *Proceedings of the National Academy of Sciences of the United States of America* **103**, 13238-13243.

Xiao, H., Radovich, C., Welty, N., Hsu, J., Li, D., Meulia, T. and van der Knaap, E. (2009) Integration of tomato reproductive developmental landmarks and expression profiles, and the effect of *SUN* on fruit shape. *Bmc Plant Biology* **9**, 49.

Yang, L., Liu, H., Zhao, J., Pan, Y., Cheng, S., Lietzow, C.D., Wen, C., Zhang, X. and Weng, Y. (2018) *LITTLELEAF* (*LL*) encodes a WD40 repeat domain-containing protein associated with organ size variation in cucumber. *Plant Journal* **95**, 834-847.

Yordanov, Y.S., Ma, C., Yordanova, E., Meilan, R., Strauss, S.H. and Busov, V.B. (2017) *BIG LEAF* is a regulator of organ size and adventitious root formation in poplar. *PLoS One* **12**, e0180527.

Zouine, M., Maza, E., Djari, A., Lauvernier, M., Frasse, P., Smouni, A., Pirrello, J. and Bouzayen, M. (2017) TomExpress, a unified tomato RNA-Seq platform for visualization of expression data, clustering and correlation networks. *Plant Journal* **92**, 727-735.

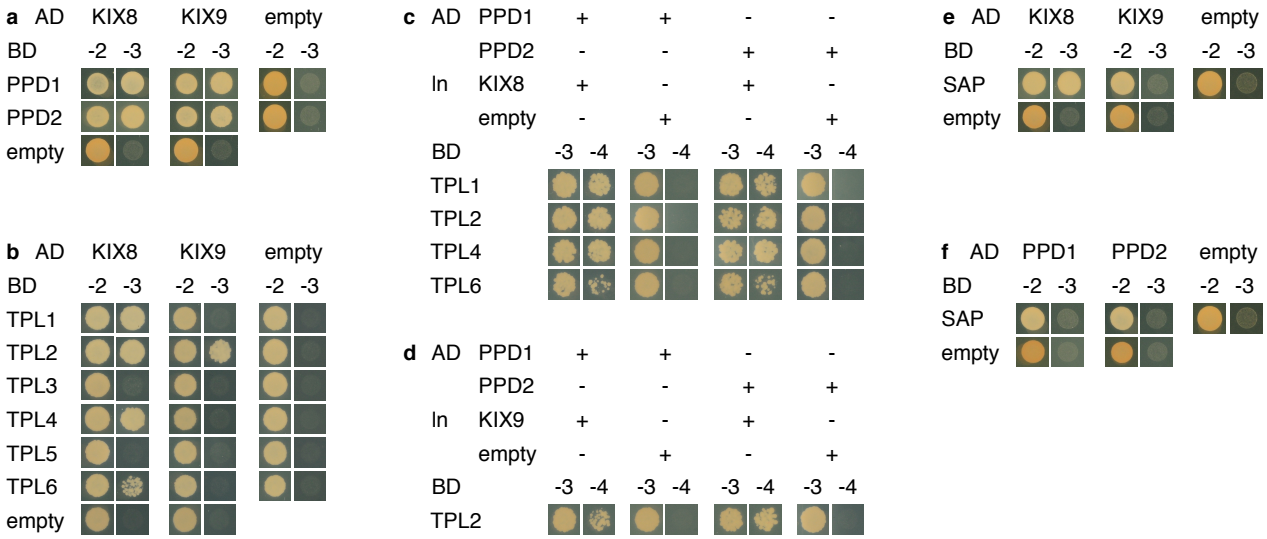

Figure 1. Tomato KIX8 and KIX9 are TPL adaptors for PPD proteins. (a−b) Y2H interaction analysis of KIX8 and KIX9 with PPD (a) and TPL (b) proteins. Yeast transformants expressing bait (BD) and prey (AD) proteins were dropped on control medium lacking Leu and Trp (−2) or selective medium additionally lacking His (−3). (c-d) Y3H interaction analysis to test the bridging capacity of KIX8 (c) and KIX9 (d) to mediate the PPD-TPL interaction. Yeast transformants expressing bait (BD), bridge (ln), and prey (AD) proteins were dropped on control medium lacking Leu, Trp, and Ura (−3) or selective medium additionally lacking His (−4). (e−f) Y2H interaction analysis of KIX (e) and PPD (f) proteins with SAP. Yeast transformants expressing bait (BD) and prey (AD) proteins were dropped on control medium lacking Leu and Trp (−2) or selective medium additionally lacking His (−3). Empty vectors were used for all control assays. Abbreviations: AD, activation domain; BD, binding domain; ln, linker.

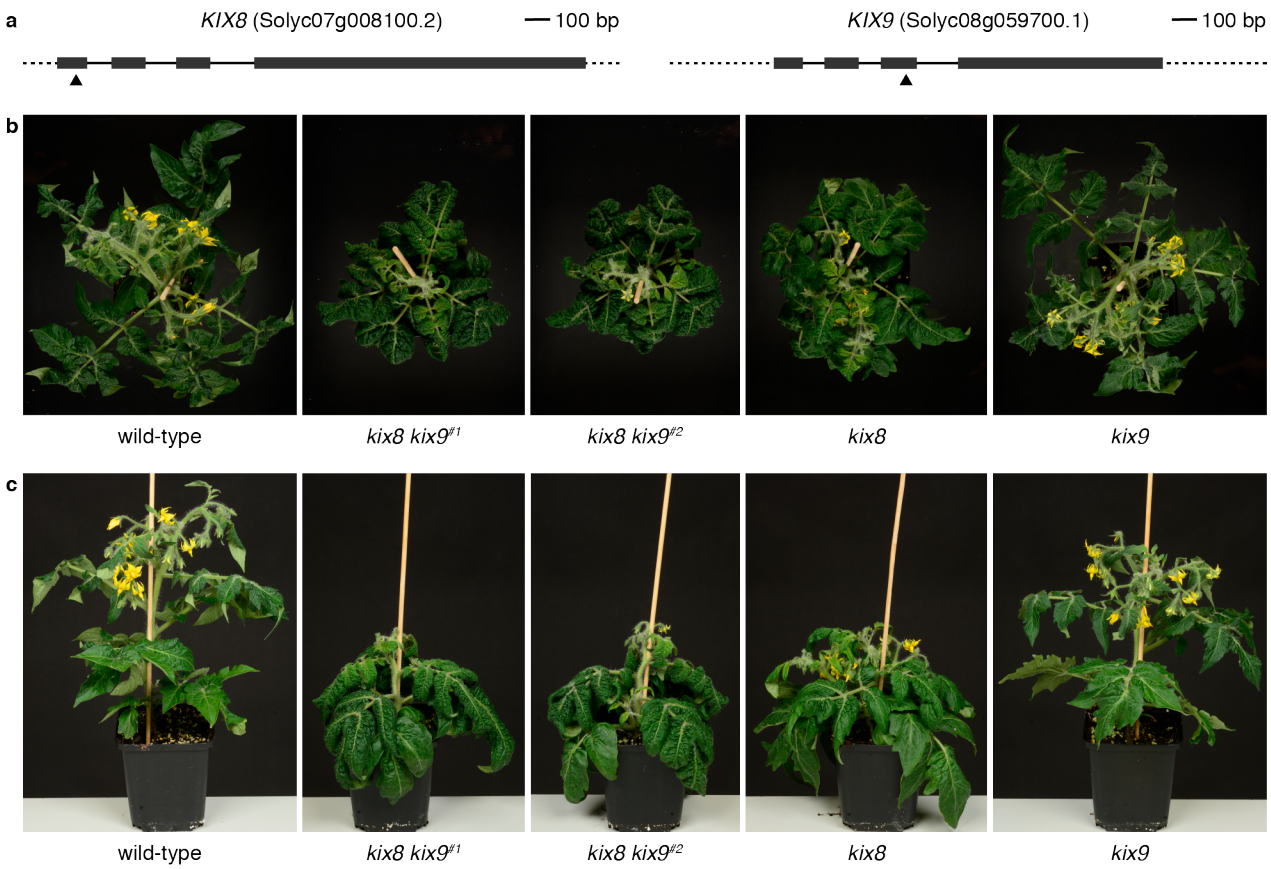

Figure 2. CRISPR-Cas9 genome editing of tomato *KIX8* and *KIX9* causes a rippled, dome-shaped leaf phenotype. (a) Schematic representation of *KIX8* and *KIX9* with location of the CRISPR-Cas9 cleavage sites. Dark grey boxes represent exons. Cas9 cleavage sites for guide RNAs are indicated with arrowheads. (b–c) Representative wild-type, *kix8 kix9*$^{\#1}$, *kix8 kix9*$^{\#2}$, *kix8*, and *kix9* plants grown in soil for 1 month under 16:8 photoperiods with daytime and nighttime temperatures of 26–29°C and 18–20°C, respectively, were photographed from the top (b) and the front (c).

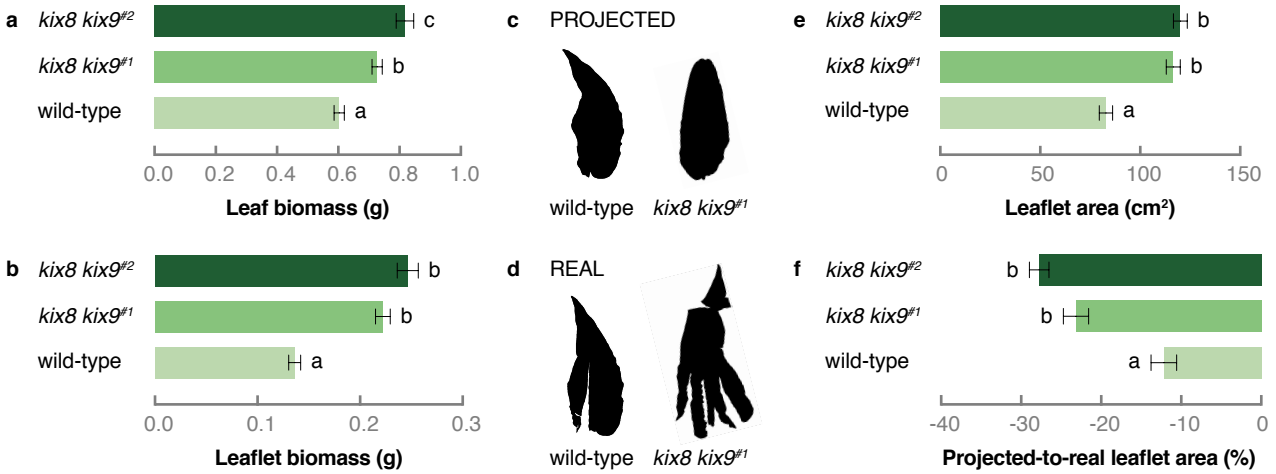

Figure 3. Tomato *kix8 kix9* plants produce enlarged, dome-shaped leaves. (a−b) Biomass of leaf eight (from the top) (a) and its terminal leaflet (b). The eighth leaf (from the top) was harvested from plants grown in soil for 2 months under 16:8 photoperiods with daytime and nighttime temperatures of 26–29°C and 18–20°C, respectively. Bars represent mean biomass relative to the mean of wild-type biomass values. Error bars denote standard error (n = 31–40). Statistical significance was determined by ANOVA followed by Tukey post-hoc analysis ($P < 0.05$; indicated by different letters). (c−d) The terminal leaflet area was measured before (projected, c) and after (real, d) the terminal leaflet of the eighth leaf was cut to flatten it. (e−f) Area (e) and projected-to-real area (f) of the terminal leaflet of the eighth leaf. Bars represent mean area relative to the mean of wild-type area values. Error bars denote standard error (n = 31–40). Statistical significance was determined by ANOVA followed by Tukey post-hoc analysis ($P < 0.05$; indicated by different letters).

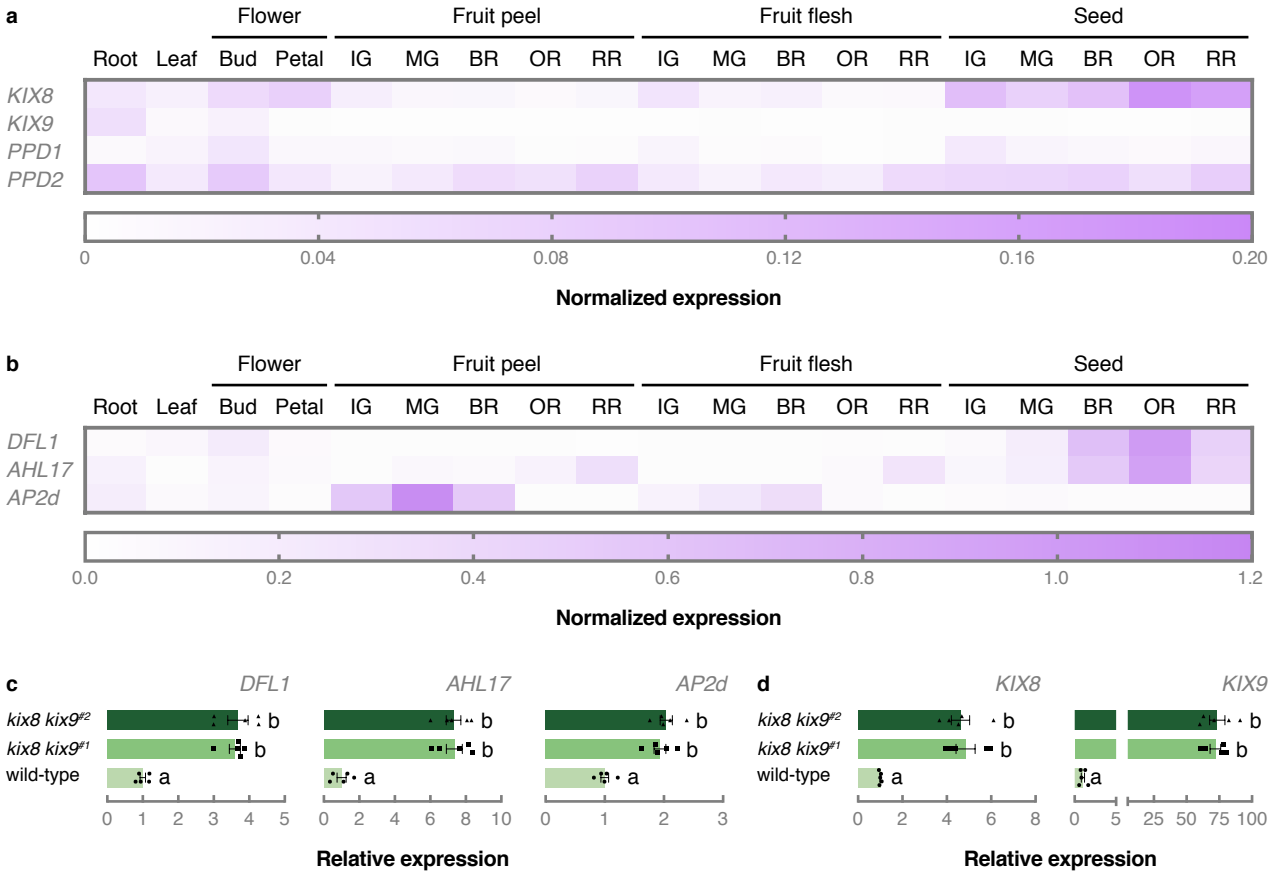

Figure 4. KIX8 and KIX9 are required for the repression of putative PPD target genes in tomato. (a−b) Normalized expression profiles of *KIX8*, *KIX9*, *PPD1*, *PPD2* (a), *DFL1*, *AHL17*, and *AP2d* (b) in different tomato organs and developmental stages (cultivar Micro-Tom). Expression data was obtained from TomExpress (Zouine *et al.*, 2017) and can be found in Table S1. (c−d) Relative expression of *DFL1*, *AHL17*, *AP2d* (c), *KIX8*, and *KIX9* (d) in terminal leaflets of not fully developed leaves analyzed by qPCR. The terminal leaflet from the second leaf (from the top) was harvested from plants grown in soil for 3 weeks under 16:8 photoperiods with daytime and nighttime temperatures of 26–29°C and 18–20°C, respectively. Bars represent mean expression relative to the mean of wild-type expression values. Error bars denote standard error (n = 5). Individual wild-type (●), *kix8 kix9*$^{\#1}$ (■), and *kix8 kix9*$^{\#2}$ (▲) values are shown. Statistical significance was determined by ANOVA followed by Tukey post-hoc analysis ($P < 0.05$; indicated by different letters). Abbreviations: IG, immature green; MG, mature green; BR, breaker; OR, orange; RR, red ripe.

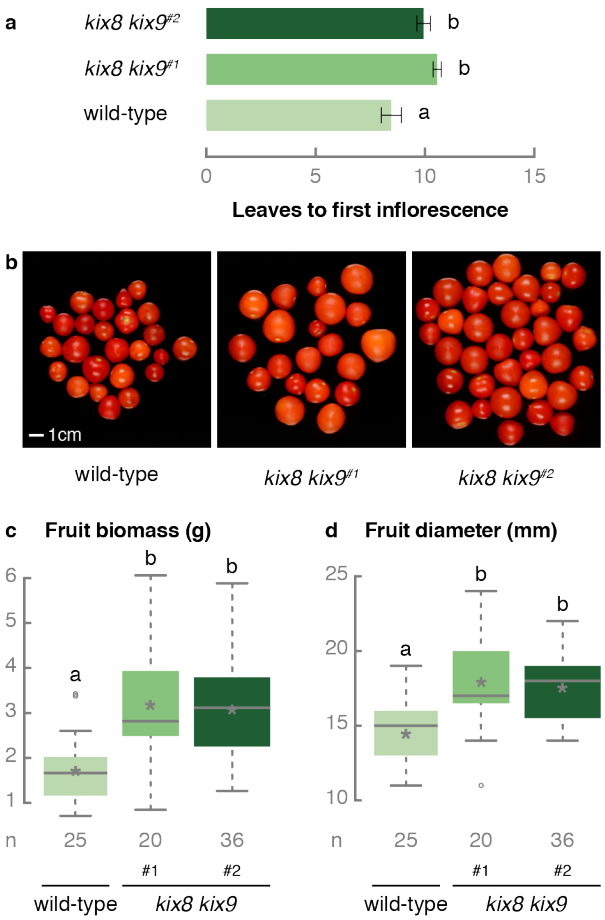

Figure 5. Tomato *kix8 kix9* plants produce bigger fruits. (a) Flowering time measured by the number of leaves produced before initiation of the first inflorescence. (b) Red ripe fruits produced by wild-type, *kix8 kix9*$^{\#1}$, and *kix8 kix9*$^{\#2}$ plants. (c–d) Biomass (c) and diameter (d) of red ripe fruits. Boxes span the interquartile range with whiskers extending 1.5 times the interquartile range. The median and mean are indicated by the center line and asterisks, respectively. Outliers are represented by open circles. Statistical significance was determined by ANOVA followed by Tukey post-hoc analysis ($P < 0.05$; indicated by different letters). For all analyses, plants were grown in soil under 16:8 photoperiods with daytime and nighttime temperatures of 26–29°C and 18–20°C, respectively.

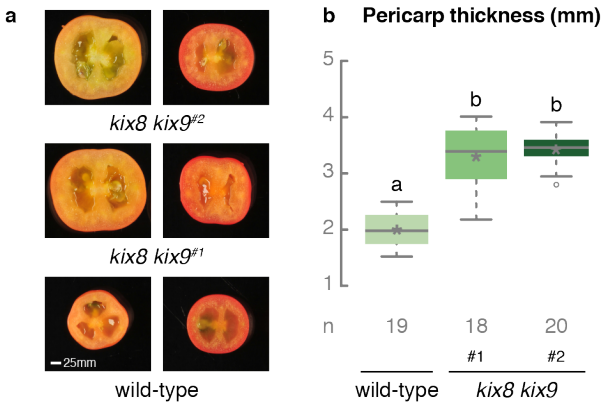

Figure 6. Fruits produced by *kix8 kix9* plants display increased pericarp thickness. (a) Equatorial sections of representative orange and red ripe fruits produced by wild-type, *kix8 kix9*$^{\#1}$, and *kix8 kix9*$^{\#2}$ plants. (b) Pericarp thickness of breaker–orange fruits. Plants were grown in soil under 16:8 photoperiods with daytime and nighttime temperatures of 26–29°C and 18–20°C, respectively. Boxes span the interquartile range with whiskers extending 1.5 times the interquartile range. The median and mean are indicated by the center line and asterisks, respectively. Outliers are represented by open circles. Statistical significance was determined by ANOVA followed by Tukey post-hoc analysis ($P < 0.05$; indicated by different letters).

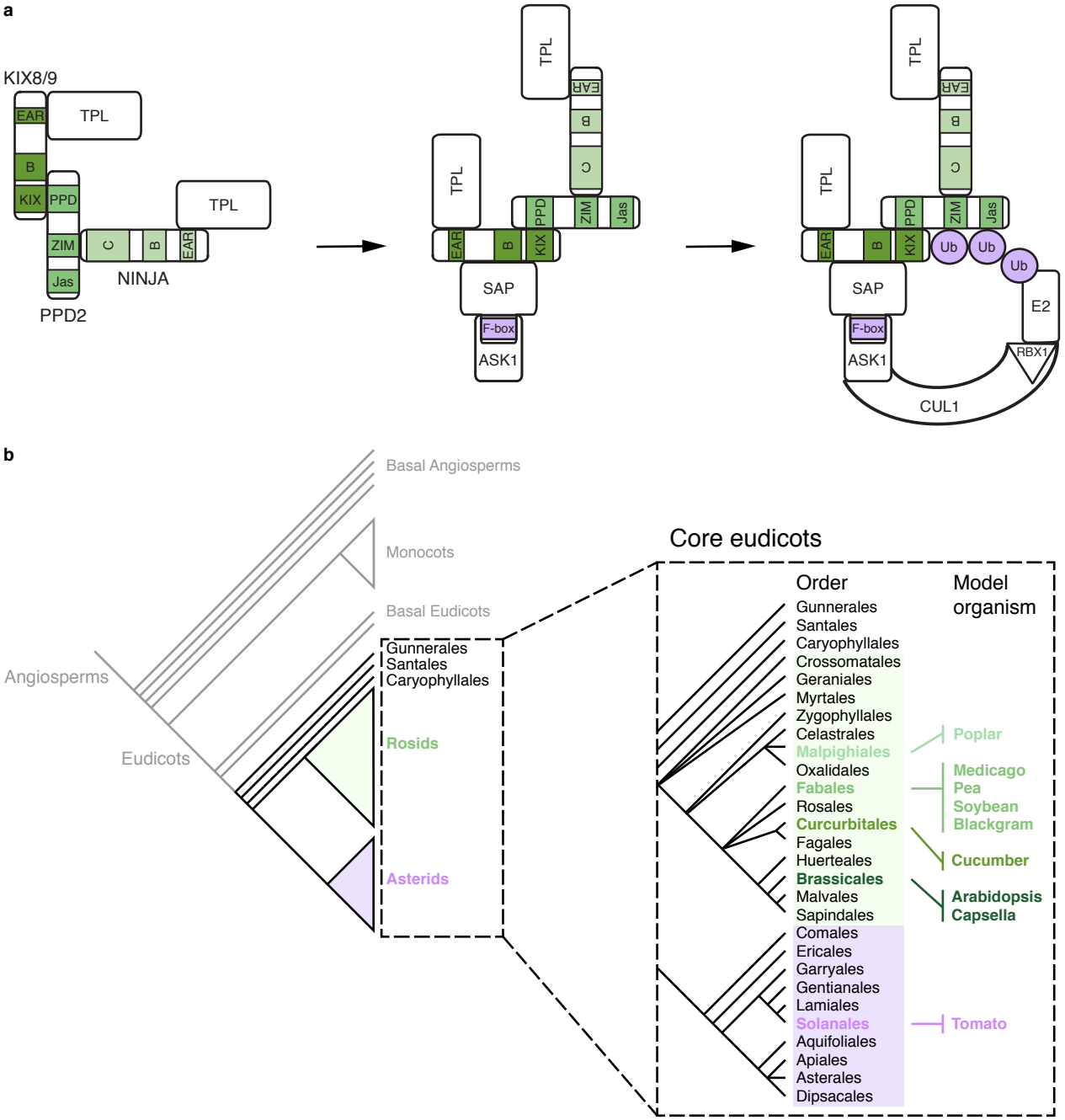

Figure S1. A conserved repressor complex regulates leaf growth in distinct eudicot species. (a) The PPD2-KIX8/KIX9 transcriptional repressor complex in *Arabidopsis thaliana*. PPD2 interacts with KIX8/KIX9 and NINJA to recruit TPL. Interaction of repressor complex members with the E3 ubiquitin ligase SCF^{SAP} (comprising the F-box protein SAP, ASK1, CUL1, and RBX1) leads to the proteasomal degradation of KIX8/KIX9 and PPD2. (b) Model organisms in which KIX, PPD and/or SAP proteins were shown to mediate leaf growth belong to different orders within the rosids, which together with the asterids, make up most of the core eudicot species. Tomato is an asterid model species in which the potential role of these proteins in regulating leaf growth has not been investigated yet. Abbreviations: ASK1, Arabidopsis SKP1; CUL1, CULLIN 1; RBX1, RING-BOX 1; SKP1, S-PHASE KINASE-ASSOCIATED PROTEIN 1; Ub, ubiquitin.

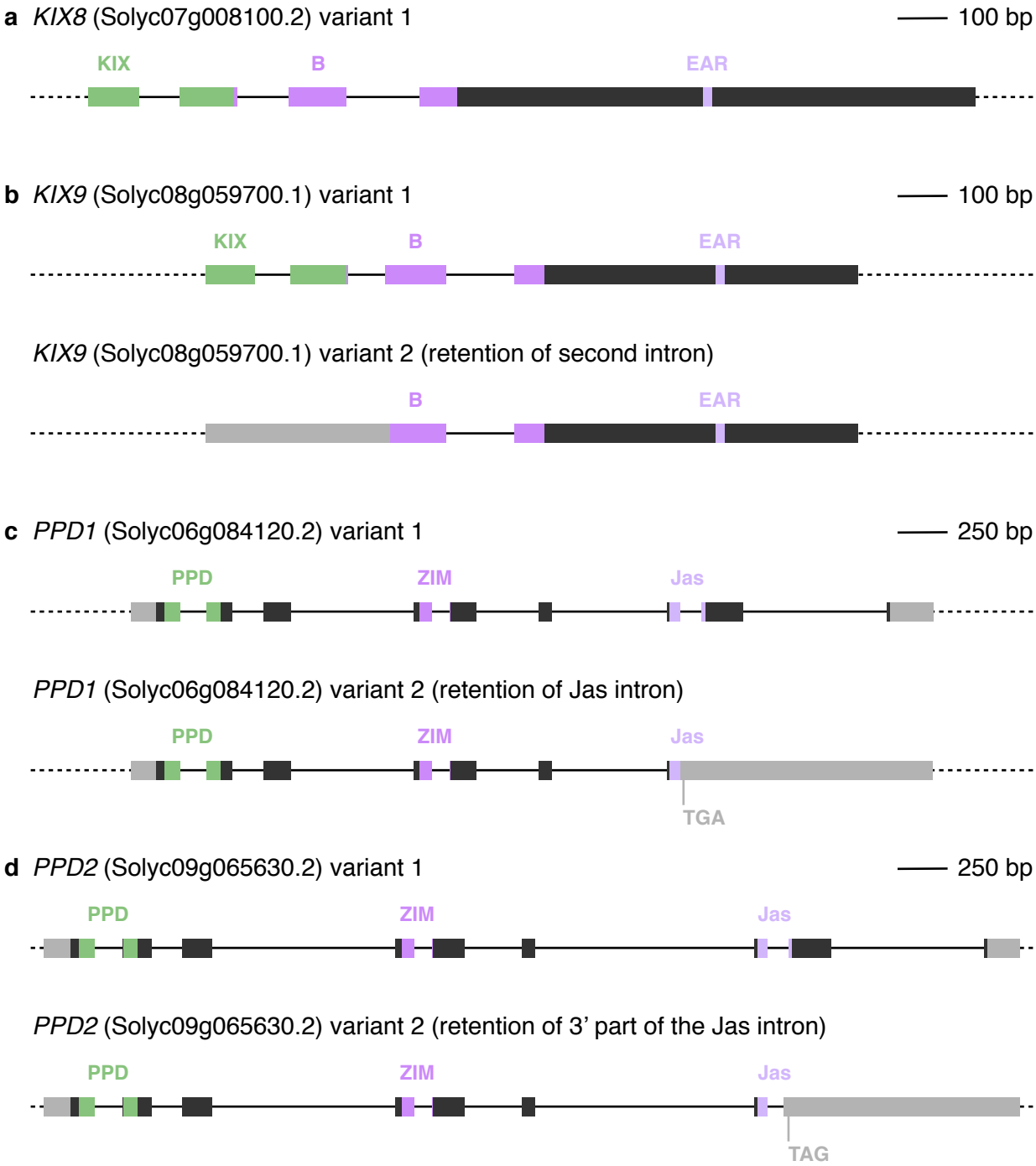

Figure S2. Splice variants of tomato *KIX8*, *KIX9*, *PPD1*, and *PPD2*. Dark grey boxes represent exons, solid lines represent introns and light grey boxes represent UTRs. Green and purple boxes represent encoded protein domains. No alternative splicing was observed for *KIX8* (a). Retention of the second *KIX9* intron (b) could lead to the use of a downstream start codon, excluding the sequence that encodes the N-terminal KIX domain. The splice variants of *PPD1* (c) and *PPD2* (d) display retention of the Jas intron and part of the Jas intron, respectively, which is located between the two exons that encode the Jas domain. These alternative splicing events generate premature stop codons. Abbreviations: UTR, untranslated region.

Figure S3. Regenerated tomato *kix8 kix9* plants display a rippled, dome-shaped leaf phenotype. (a–b) Wild-type and regenerated *kix8 kix9* plants were photographed from the front (a) and the top (b). Primary transformants transferred from rooting medium were grown in soil for 10 weeks under 16:8 photoperiods with daytime and nighttime temperatures of 26–29°C and 18–20°C, respectively.

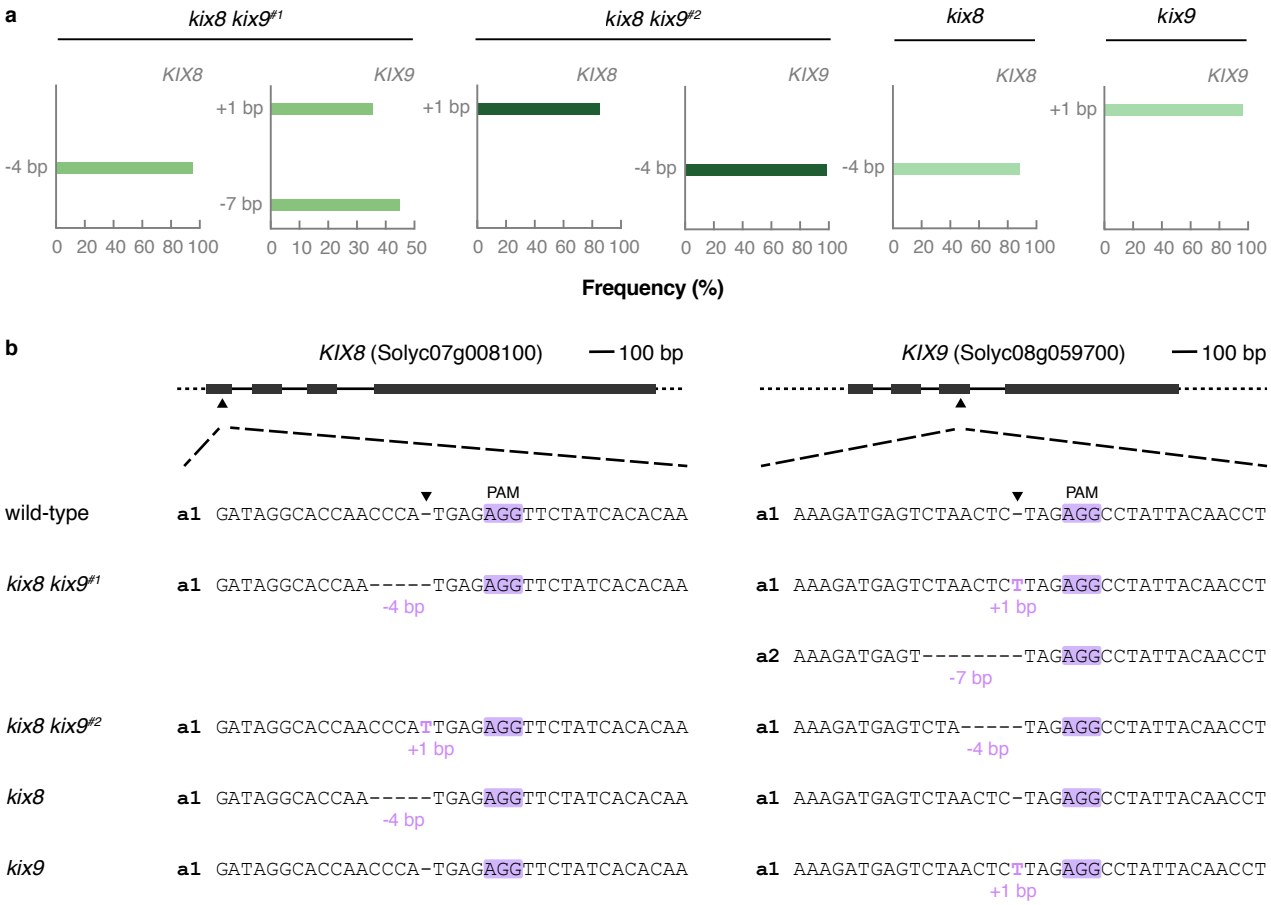

Figure S4. CRISPR-Cas9 mutations in tomato double *kix8 kix9* (T1) and single *kix8* and *kix9* knockout lines. (a) ICE analysis of genomic sites targeted by the guide RNAs. Targeted genomic regions were PCR amplified and sequenced by Sanger sequencing. Based on the sequence chromatograms, ICE analysis visualized the indel spectrum and calculated the frequency of each indel. (b) Schematic representation of *KIX8* and *KIX9* with location of the CRISPR-Cas9 cleavage sites. Dark grey boxes represent exons and solid lines represent introns. Cas9 cleavage sites for guide RNAs are indicated with arrowheads. Allele sequences are shown for two independent *kix8 kix9* lines and one *kix8* and one *kix9* line. Abbreviations: a, allele; PAM, protospacer adjacent motif.

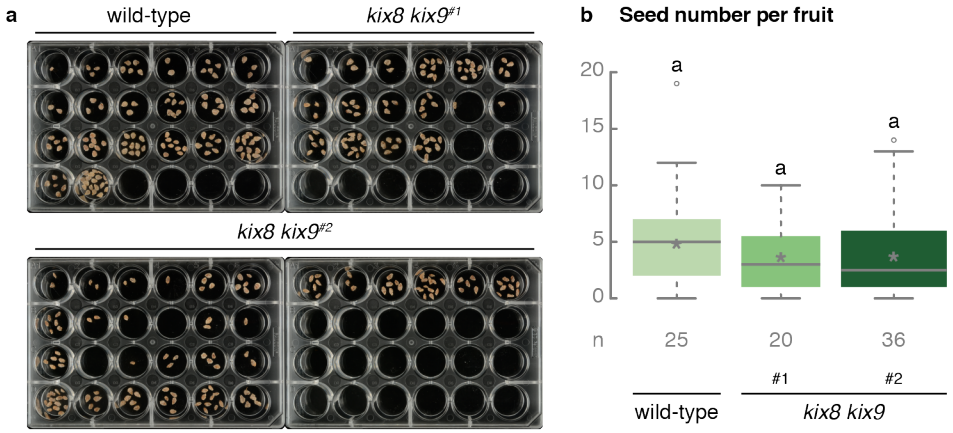

Figure S5. Tomato *kix8 kix9* plants do not exhibit a seed phenotype. (a) Seeds produced by wild-type, *kix8 kix9*$^{\#1}$, and *kix8 kix9*$^{\#2}$ plants. Each well contains the seeds produced by a single fruit. (b) Number of seeds produced by wild-type, *kix8 kix9*$^{\#1}$, and *kix8 kix9*$^{\#2}$ plants. Boxes span the interquartile range with whiskers extending 1.5 times the interquartile range. The median and mean are indicated by the center line and asterisks, respectively. Outliers are represented by open circles. Statistical significance was determined by ANOVA followed by Tukey post-hoc analysis ($P < 0.05$; indicated by different letters). Plants were grown in soil under 16:8 photoperiods with daytime and nighttime temperatures of 26–29°C and 18–20°C, respectively.

Table S1. Normalized expression of *KIX8*, *KIX9*, *PPD1*, *PPD2*, *DFL1*, *AHL17*, and *AP2d* in different tomato organs and developmental stages (cultivar Micro-Tom) used to draw heat maps in Figure 4a–b

			Flower		Fruit peel					Fruit flesh					Seed				
	Root	Leaf	Bud	Petal	IG	MG	BR	OR	RR	IG	MG	BR	OR	RR	IG	MG	BR	OR	RR
KIX8	0.040	0.022	0.061	0.079	0.026	0.011	0.013	0.006	0.0134	0.044	0.018	0.022	0.008	0.009	0.120	0.078	0.103	0.179	0.158
KIX9	0.053	0.008	0.021	0	0	0	0	0	0	0	0.001	0	0	0	0.001	0.001	0	0	0
PPD1	0.006	0.017	0.041	0.010	0.010	0.006	0.010	0	0	0.020	0.003	0.005	0	0.002	0.035	0.015	0.011	0.006	0.012
PPD2	0.098	0.035	0.090	0.039	0.020	0.034	0.060	0.050	0.080	0.040	0.020	0.037	0.029	0.061	0.066	0.069	0.074	0.053	0.082
DFL1	0.031	0.067	0.190	0.033	0.007	0.011	0	0	0	0.010	0.007	0.007	0.019	0.004	0.049	0.165	0.633	0.980	0.450
AHL17	0.123	0	0.098	0.043	0.010	0.065	0.040	0.110	0.310	0.010	0.017	0.015	0.041	0.253	0.071	0.158	0.533	0.925	0.405
AP2d	0.164	0.046	0.092	0.024	0.542	1.108	0.520	0	0	0.120	0.223	0.323	0.036	0.003	0.032	0.038	0.019	0.023	0.025

Expression data was obtained from TomExpress (Zouine *et al.*, 2017). Abbreviations: IG, immature green; MG, mature green; BR, breaker; OR, orange; RR, red ripe.

Table S2. Oligonucleotides used in this study

Oligonucleotide	Sequence (5'–3')	Orientation	Description	SolycID
Oligonucleotides for Y2H/Y3H constructs:				
LAPAU2860	GGGGACAAGTTTGTACAAAAAAGCAGGCTCCATGCCTAGACCAGGACCCAG	Forward	amplification of *KIX8*	Solyc07g008100.2
LAPAU2994	GGGGACCACTTTGTACAAGAAAGCTGGGTCTCMCAAACCTGGCCTTTTCATTTG	Reverse		
LAPAU2862	GGGGACAAGTTTGTACAAAAAAGCAGGCTCCATGCCTAAATCTACAAGAGC	Forward	amplification of *KIX9*	Solyc08g059700.1
LAPAU2863	GGGGACCACTTTGTACAAGAAAGCTGGGTCTCMGGACTTGAATTTGTTAAAATG	Reverse		
LAPAU2856	GGGGACAAGTTTGTACAAAAAAGCAGGCTCCATGCCGCCGGAAGAAACAG	Forward	amplification of *PPD1*	Solyc06g084120.2
LAPAU2857	GGGGACCACTTTGTACAAGAAAGCTGGGTCTCMCTTTCTAACATCTCTGTC	Reverse		
LAPAU2858	GGGGACAAGTTTGTACAAAAAAGCAGGCTCCATGTCGCTGGAACAAACTG	Forward	amplification of *PPD2*	Solyc09g065630.2
LAPAU2859	GGGGACCACTTTGTACAAGAAAGCTGGGTCTCMCTCTTTACCATCTTTG	Reverse		
COMBI6198	GGGGACAAGTTTGTACAAAAAAGCAGGCTCCATGTCGTCTTCACAATCACCACCATC	Forward	amplification of *SAP*	Solyc05g041220.2
COMBI6199	GGGGACCACTTTGTACAAGAAAGCTGGGTTCACTATTGTGCACCAAAGTCCCACAAATG	Reverse		
Oligonucleotides for CRISPR-Cas9 constructs:				
LAPAU2582	ATTGATAGGCACCAACCCATGAG	Forward	*KIX8* gRNA target site	Solyc07g008100.2
LAPAU2583	AAACCTCATGGGTTGGTGCCTAT	Reverse		
LAPAU2580	ATTGAAAGATGAGTCTAACTCTAG	Forward	*KIX9* gRNA target site	Solyc08g059700.1
LAPAU2581	AAACCTAGAGTTAGACTCATCTTT	Reverse		
Oligonucleotides for the identification of CRISPR-Cas9 mutants:				
LAPAU3075	TCCCTCATCAGATCCACCTC	Forward	amplification of *Cas9*	–
LAPAU3076	CTGAAACCTGAGCCTTCTGG	Reverse		
LAPAU2783	CCCCTCCAAAACACTCATGT	Forward	amplification of *KIX8* gRNA target region	Solyc07g008100.2
LAPAU2784	GAGCAGTACAAATGAGCAGCA	Reverse		
LAPAU2785	GCTGAAGAAATTATGTATTCCAAAGC	Forward	amplification of *KIX9* gRNA target region	Solyc08g059700.1
LAPAU2786	CCCGAGAAGTTTCACTCGAA	Reverse		
Oligonucleotides for gene expression analysis by qPCR:				
COMBI5428	CCTCCGTTGTGATGTAACTGG	Forward	amplification of *CAC*	Solyc08g006960.2
COMBI5429	ATTGGTGGAAAGTAACATCATCG	Reverse		
COMBI5416	ATGGAGTTTTTGAGTCTTCTGC	Forward	amplification of *TIP41*	Solyc10g049850.1
COMBI5417	GCTGCGTTTCTGGCTTAGG	Reverse		
COMBI7162	ACCATCGAAGAGTCTCTCAACAGC	Forward	amplification of *DFL1*	Solyc07g063850.2
COMBI7163	CAATGGATTTGTCTGAGGCACGAC	Reverse		
COMBI7168	CTGTCATTTGCCGTCGGATGTG	Forward	amplification of *AHL17*	Solyc04g076220.2
COMBI7169	AGTAAGGCGGTGGTTGTGGTTG	Reverse		
COMBI7158	TGCATAGTCAGGTCGGAACAACG	Forward	amplification of *AP2d*	Solyc11g072600.1
COMBI7159	TGGTAGCCGGAGTTGAGAATCC	Reverse		

COMBI7188	AGGCTGTGTCTACCAGCAAAGAC	Forward	amplification of *KIX8*	Solyc07g008100.2
COMBI7189	TTGCAACCCGGAGTGACTGTTG	Reverse		
COMBI7190	AGACACCAACCAATCAGAGGTTCC	Forward	amplification of *KIX9*	Solyc08g059700.1
COMBI7191	TGCTGAGCCATGAACCTCATTCAC	Reverse		